

Photolithographic patterning of vacuum-deposited organic light emitting devices

P. F. Tian, P. E. Burrows, and S. R. Forrest

*Department of Electrical Engineering, Center for Photonics and Optoelectronic Materials,
Princeton University, Princeton, New Jersey 08544*

(Received 4 August 1997; accepted for publication 30 September 1997)

We demonstrate a photolithographic technique to fabricate vacuum-deposited organic light emitting devices. Photoresist liftoff combined with vertical deposition of the emissive organic materials and the metal cathode, followed by oblique deposition of a metal cap, avoids the use of high processing temperatures and the exposure of the organic materials to chemical degradation. The unpackaged devices show no sign of deterioration in room ambient when compared with conventional devices fabricated using low-resolution, shadow mask patterning. Furthermore, the devices are resistant to rapid degradation when operated in air for extended periods. This work illustrates a potential foundation for the volume production of very high-resolution, full color, flat panel displays based on small molecular weight organic light emitting devices. © 1997 American Institute of Physics. [S0003-6951(97)01848-2]

Organic light emitting devices (OLEDs) are attracting attention for potential use in flat panel displays (FPDs) due to their high efficiency,¹ long lifetime,^{2,3} low driving voltage, wide viewing angle, light weight, and potential low cost.⁴⁻⁶ High resolution patterning, one of the key manufacturing challenges leading to the practical commercialization of full color flat panel displays,⁴ has yet to be demonstrated using OLEDs based on either polymers or small molecular weight vacuum-deposited thin films.

A typical small molecular weight OLED consists of two or more layers of organic materials sandwiched between a transparent indium tin oxide (ITO) anode coated on a glass substrate, and a metal cathode such as an alloy of Mg and Ag.⁷ Both top and bottom electrodes need to be patterned to form OLEDs less than 100 μm in diameter to achieve high-resolution and full color FPDs. While the bottom ITO electrode is easily patterned using a combination of standard photolithography and wet chemical etching, the top electrode is typically defined by deposition through a shadow mask, resulting in a minimum practical pattern dimension of $\sim 200\text{--}300\text{ }\mu\text{m}$. If three adjacent red, green, and blue subpixels are required to achieve full color, precise shadow mask alignment becomes a limiting factor, leading to pixel dimensions of $\sim 1\text{ mm}$ which is too large for use in high-resolution FPDs. Furthermore, shadow masking has the disadvantage of requiring frequent mask replacement or cleaning to maintain high dimensional control of the underlying display panel. Thus, for most practical manufacturing purposes, a suitable method needs to be established to microfabricate the top cathode.

Previously, an array of $20\text{ }\mu\text{m}\times 20\text{ }\mu\text{m}$ active region polymer OLEDs placed on $40\text{ }\mu\text{m}$ centers was fabricated by excimer laser photoablation of both the ITO anode and metal cathode.⁸ Although this pixel dimension is suitable for high-resolution displays, laser ablation may not be capable of volume production of large screen displays due to its low speed. Hence, photolithographic patterning is potentially most suitable for the microfabrication of OLEDs since it provides high resolution, it can be used to handle large panels, and is

potentially compatible with the fabrication of the OLED driving circuits.

To date, however, the photolithographic patterning of small molecular weight OLEDs has been very difficult due to the degradation or complete failure of the devices after being exposed to water vapor, O_2 , or solvents and developers used in the removal and patterning of photoresists.⁹⁻¹³ Thus, device encapsulation and/or dry processing techniques are necessary. To avoid wet processing of the organic materials, thick insulator walls combined with the evaporation of cathode materials at a suitable angle were proposed to micropattern the cathode contacts.¹⁴⁻¹⁶ Recently, such micropatterned cathodes were demonstrated by using thick photoresist strips in a multicolor OLED display,¹⁷ thereby exposing the edges of the active organic materials to chemical attack upon subsequent processing. In this work we describe a photolithographic method to pattern top cathodes at high resolution and high device yield without damaging either the materials or device properties. Furthermore, the completed devices are encapsulated by a metal cap, making them particularly resistant to attack from environmental contaminants.

The patterned OLEDs were fabricated following the process shown schematically in Fig. 1. Prior to thin film deposition, glass substrates precoated with ITO ($10\text{ }\Omega/\square$) were cleaned by sequential ultrasonic agitation, boiling in solvents (1, 1, 1-trichloroethane, acetone and 2-propanol, respectively) and then blown dry in pure N_2 . Next, a 2000-\AA -thick polyimide layer was spun on the substrate from a dilute Pro-bimide 285 (Olin Microelectronic Materials) solution and cured in atmosphere. This was followed by standard photolithographic patterning and exposure to O_2 plasma reactive ion etching for 5 min at 50 W and 100 mTorr to expose the ITO contact, thus defining the OLED active region dimension of $300\text{ }\mu\text{m}\times 1.5\text{ mm}$ spaced on $500\text{ }\mu\text{m}$ centers. This was followed by deposition of a $2\text{-}\mu\text{m}$ -thick SiO_2 layer using plasma-enhanced chemical vapor deposition with SiH_4 and N_2O gas sources at $280\text{ }^\circ\text{C}$. Next, a $2\text{-}\mu\text{m}$ -thick photoresist (AZ4210) layer was spun on and patterned using a second mask consisting of $400\text{ }\mu\text{m}\times 1\text{ cm}$ strips centered over the

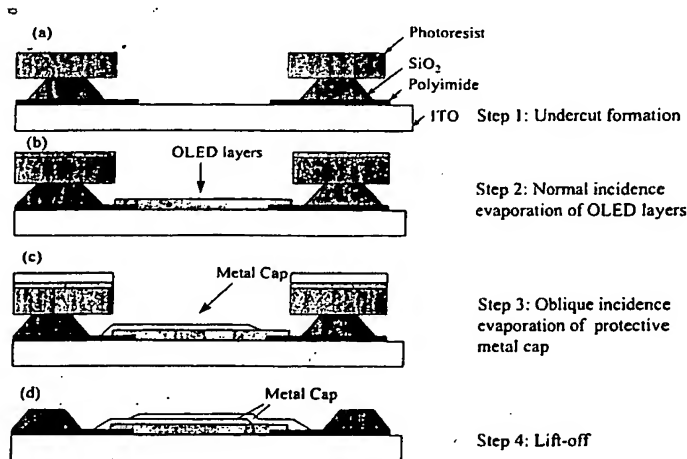


FIG. 1. Schematic diagram of steps used in the photolithographic patterning of vacuum-deposited, small molecular weight OLEDs.

holes in the polyimide layer. Undercuts were formed by wet etching the SiO₂ layer using a mixture of buffered oxide etchant (10:1) and HF (49%) with a volume ratio of 10:1 for ~3.4 min [Fig. 1(a)]. Next, the OLED layers were evaporated in vacuum under a base pressure of 3×10^{-6} Torr through the photoresist patterns in a direction normal to the substrate plane [Fig. 1(b)]. The growth sequence of these layers was as follows: a 400-Å-thick α -NPD hole transport layer was deposited, followed by deposition of a 600-Å-thick Alq₃ layer which served as both the light emitting and electron transport material. Next, a 250-Å-thick Mg:Ag cathode with an atomic ratio of 24:1 was co-evaporated, followed by the deposition of a 200-Å-thick Ag protection layer. Then, a 0.5- μ m-thick Ag layer was obliquely deposited onto the stationary substrate to cover one side of the devices [Fig. 1(c)], followed by rotating the substrate 180° and evaporating another 0.5 μ m Ag to cover the opposite side of the devices. This process can be simplified by installing a planetary mount into the vacuum chamber which allows for substrate rotation during deposition. Finally, lift-off of the photoresist mask was accomplished by soaking in acetone for several minutes, followed by drying in pure N₂ [Fig. 1(d)].

Figure 2 shows an optical micrograph of an array of seven patterned devices. The narrow black strips separating

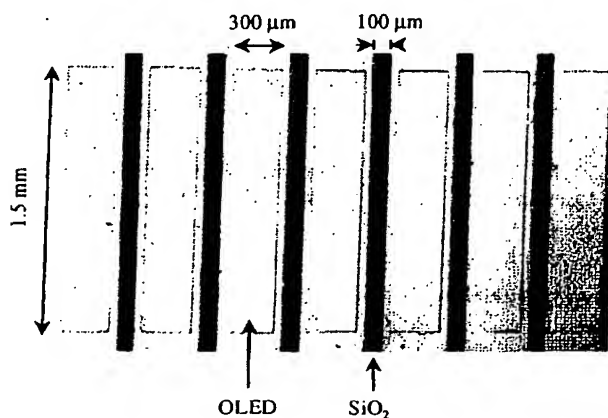


FIG. 2. Optical micrograph of the completed, photolithographically patterned devices.

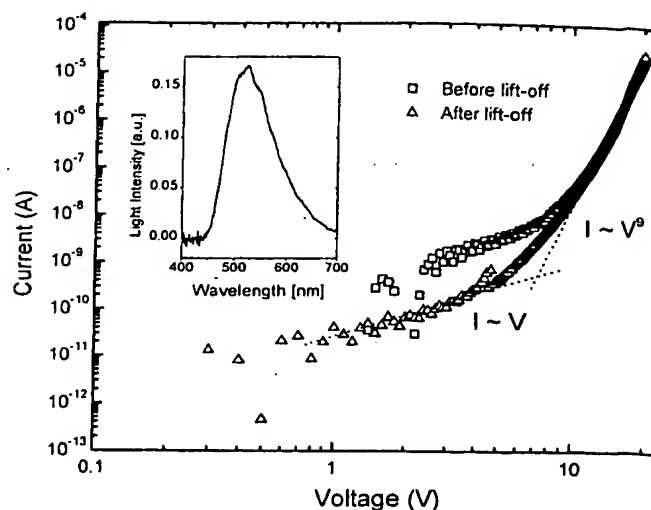


FIG. 3. Current vs voltage characteristics of a 0.45 mm² device obtained prior to and after photoresist liftoff in acetone. Inset: Electroluminescence spectrum of the patterned device.

the device contacts are the SiO₂ isolation regions. The wide gray strips are the Ag caps, with the raised portion of the contact corresponding to the OLED active regions. The overall smooth appearance of the devices indicates no obvious solvent penetration into the organic materials due to complete sealing by the metal cap. A few physical defects observed are possibly caused by particles preexisting on the ITO-coated substrate, or introduced during subsequent film deposition. These defects can be reduced or eliminated by careful substrate cleaning and proper handling in a suitable clean process environment.

The lack of solvent penetration is also inferred by comparing the forward bias current-voltage (I - V) characteristics of the devices before and after liftoff, as shown in Fig. 3. Both characteristics are similar to those previously reported for conventional devices.¹⁸ We note, however, that a few of the devices were shorted before liftoff possibly due to metal bridges causing shorts between the metal on the photoresist surfaces and the device caps. After liftoff, however, all devices were electrically isolated. At low voltages, $I \sim V$ indicating ohmic conduction; whereas at high voltages, $I \sim V^6$ implying trapped-charge-limited conduction.¹⁸ The device turn-on voltages demonstrating the transition from ohmic to trap-limited conduction are between 6 and 7 V. These data suggest that there is no degradation of the I - V characteristics due to the lift-off process. The inset of Fig. 3 shows the electroluminescence spectrum of a device after liftoff. This spectrum is also similar to that of conventional devices fabricated using shadow mask techniques.¹⁸

Figure 4 shows the light output versus current (L - I) characteristics for devices prior to and after liftoff. The external quantum efficiencies measured only in the forward scattered direction are ~0.6%, typical of undoped Alq₃-based OLEDs. Again, we find no apparent differences between devices characterized before and after liftoff. Approximately 70% of the devices after liftoff were defect-free, exhibiting I - V and L - I characteristics as shown in Figs. 3 and 4. The remaining 30% either had a low quantum efficiency or did not emit light due to defects. We anticipate the

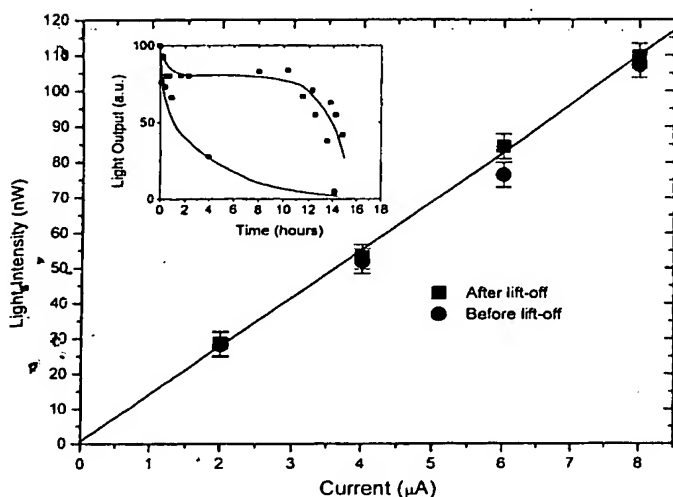


FIG. 4. Light output vs current characteristics of a 0.45 mm^2 device obtained prior to and after liftoff. Inset: Time evolution of the light output of the cathode patterned device at a constant current density of 6.4 mA/cm^2 (squares), and of the conventional unpackaged 0.1 cm^2 devices fabricated using shadow mask technique at a constant current density of 10 mA/cm^2 (circles). The initial luminance was 130 cd/m^2 for patterned device and 30 cd/m^2 for the conventional devices.

yield will approach 100% if the ITO surface is properly prepared to remove defects and particles prior to device fabrication.

The inset of Fig. 4 shows the time evolution ($L-t$) of light output from a typical, unpackaged patterned device (squares) obtained at a constant current density of 6.4 mA/cm^2 . Prior to the test, the devices were exposed to air (humidity $\sim 60\%$) at room temperature for approximately 100 h. The lifetime, defined as the time at which the luminance drops to half of its initial value, was $\sim 14 \text{ h}$. Failure of the device was due to the appearance of a $300\text{-}\mu\text{m}$ -diam dark spot, which again is attributed to particles on the ITO surface. The time evolution of the average light output of unpackaged devices fabricated using conventional shadow mask method (circles) is also shown for comparison in the inset of Fig. 4.¹⁹ These devices, which were tested immediately after fabrication, had a lifetime of $\sim 2 \text{ h}$. Both tests were performed at room ambient and temperature. In contrast to the patterned OLEDs, prolonged exposure of unpackaged, conventional devices is found to lead to rapid degradation and a "shelf life" of only several hours. Although more systematic studies are required, we infer from these data that the unpackaged patterned devices probably have significantly longer shelf and operational lifetimes than unpackaged conventional OLEDs. We emphasize, however, that all practical devices must be placed in a sealed package to ensure very long term operational lifetime. The benefit of the environmental robustness of the encapsulated devices is that it allows for continued exposure of devices to the environment should subsequent device processing or handling be required prior to packaging.

The ultimate resolution achievable using the process

in Fig. 1 is estimated to be equal to the active region diameter $+ 2 \times (\text{undercut gap} + \text{insulator pattern tolerance}) + \text{SiO}_2$ width. Since the undercut gap is equal to or larger than the SiO_2 thickness, a reasonable estimate of the minimum device spacing is the pixel active region diameter plus $15 \text{ }\mu\text{m}$. For a high definition display with an active pixel diameter of $85 \text{ }\mu\text{m}$, a pixel separation of $100 \text{ }\mu\text{m}$ is required, leading to an aperture ratio of 85%. Both the resolution and aperture ratio can be further improved by refining the photolithographic techniques discussed here.

In conclusion, we have demonstrated a simple photolithographic method capable of microfabricating vacuum-deposited, small molecular weight organic devices, such as OLEDs, without apparent damage to the devices. The OLEDs are encapsulated by a thick inactive metal layer, significantly increasing shelf and operational lifetimes. The extended shelf life is important if the devices require subsequent processing steps after patterning as is the case for adjacent positioning of red, green, and blue OLEDs in a full color display. This simple patterning technique illustrates a potential foundation for the volume production of very high-resolution, multicolor flat-panel displays or other active optoelectronic devices based on small molecular weight vacuum-deposited organic thin films.

The authors thank G. Gu for his assistance in lifetime tests, and H. Uenohara, V. Bulovic, and M. Valenti for helpful discussions. They are grateful to Universal Display Corp. and DARPA/Wright Labs for their generous support of this work.

- ¹ S. A. VanSlyke and C. W. Tang, 1995 Digest of LEOS Summer Topical Meetings, 1995, p. 3.
- ² J. Shi and C. W. Tang, Appl. Phys. Lett. **70**, 1665 (1997).
- ³ S. A. VanSlyke, C. H. Chen, and C. W. Tang, Appl. Phys. Lett. **69**, 2160 (1996).
- ⁴ L. J. Rothberg and A. J. Lovinger, J. Mater. Res. **11**, 3174 (1996).
- ⁵ P. E. Burrows, S. R. Forrest, and M. E. Thompson, Current Opinion in Solid State & Materials Science **2**, 236 (1997).
- ⁶ S. R. Forrest, P. E. Burrows, and M. E. Thompson, Laser Focus World **99**, Feb. (1995).
- ⁷ C. W. Tang and S. A. VanSlyke, Appl. Phys. Lett. **51**, 913 (1987).
- ⁸ S. Noach, E. Z. Faraggi, G. Cohen, Y. Avny, R. Neumann, D. Davidov, and A. Lewis, Appl. Phys. Lett. **69**, 3650 (1996).
- ⁹ D. Yap, P. E. Burrows, and S. R. Forrest, Organic Thin Films for Photonics Applications, Technical Digest, 1995, p. 302.
- ¹⁰ R. B. Taylor, P. E. Burrows, and S. R. Forrest, IEEE Photonics Technol. Lett. **9**, 365 (1997).
- ¹¹ C. C. Wu, J. C. Sturm, R. A. Register, and M. E. Thompson, Appl. Phys. Lett. **69**, 3117 (1996).
- ¹² D. G. Lidzey, M. A. Pate, M. S. Weaver, T. A. Fisher, and D. D. C. Bradley, Synth. Met. **82**, 141 (1996).
- ¹³ F. Papadimitrakopoulos, X. Zhang, D. L. Thomsen, and K. A. Higginson, Chem. Mater. **8**, 1363 (1996).
- ¹⁴ C. W. Tang, U.S. Patent No. 5 276 380.
- ¹⁵ C. W. Tang and J. E. Littman, U.S. Patent No. 5 294 869.
- ¹⁶ C. W. Tang, D. J. Williams, and J. C. Chang, U.S. Patent No. 5 294 870.
- ¹⁷ C. Hosokawa, M. Eida, M. Matsuura, K. Fukuoaka, H. Nakamura, and T. Kusumoto, SID 97 Digest, 1997 p. 1073.
- ¹⁸ P. E. Burrows, Z. Shen, V. Bulovic, D. M. McCarty, S. R. Forrest, J. A. Cronin, and M. E. Thompson, J. Appl. Phys. **10**, 79 (1996).
- ¹⁹ P. E. Burrows, V. Bulovic, S. R. Forrest, L. S. Sapochak, D. M. McCarty, and M. E. Thompson, Appl. Phys. Lett. **65**, 2922 (1994).